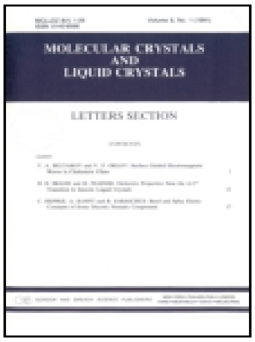

Taylor & Francis
Taylor & Francis Group

Molecular Crystals and Liquid Crystals

ISSN: 1542-1406 (Print) 1563-5287 (Online) Journal homepage: http://www.tandfonline.com/loi/gmcl20

Prediction of crystal morphology of 1,3,5-triamino-2,4,6-trinitrobenzene in dimethyl sulfoxide via modified attachment energy modeling and its experimental validation

Jian Liu, Jie Sun, Haobing Zhang & Yushi Wen

To cite this article: Jian Liu, Jie Sun, Haobing Zhang & Yushi Wen (2016) Prediction of crystal morphology of 1,3,5-triamino-2,4,6-trinitrobenzene in dimethyl sulfoxide via modified attachment energy modeling and its experimental validation, Molecular Crystals and Liquid Crystals, 634:1, 97-103, DOI: 10.1080/15421406.2016.1177910

To link to this article: http://dx.doi.org/10.1080/15421406.2016.1177910

MOLECULAR CRYSTALS AND LIQUID CRYSTALS
2016, VOL. 634, 97–103
http://dx.doi.org/10.1080/15421406.2016.1177910

Prediction of crystal morphology of 1,3,5-triamino-2,4,6-trinitrobenzene in dimethyl sulfoxide via modified attachment energy modeling and its experimental validation

Jian Liu, Jie Sun, Haobing Zhang, and Yushi Wen

Institute of Chemical Materials, China Academy of Engineering Physics, Mianyang, China

ABSTRACT
A new computational method was established to investigate the solvent effects on the crystal morphology of 1,3,5-triamino-2,4,6-trinitrobenzene (TATB). The modified attachment energy (MAE) method was applied on TATB in dimethyl sulfoxide (DMSO). This MAE E_{satt} method accounting for the attachment energy effect of the solvent was proposed to replace the vacuum attachment energy using the solvent-crystal interaction energies. In our simulation study, TATB crystals in DMSO grew into a hexagonal-flake structure and are in good agreement with the experimental data.

KEYWORDS
Modified attachment energy; morphology; TATB

1. Introduction

The crystal morphology of explosive has a direct effect on their physical properties such as fluidity, packing density, and electrostatic accumulation and even has a significant effect on the stability, detonation ability, and sensitivity of explosives [1, 2]. As for the packing density, the needle-like and plate-like crystals have unexpected shapes resulting in high density. In addition, isometric crystals also have higher density [3]. Thus, the investigations on the crystal morphology control are important for energetic materials.

Molecular modeling offers methods to predict the steady state crystal shapes under various conditions. The relationship between the apparent structure of a crystal and its internal molecular arrangement was initially investigated by Bravais, Friedel, Donnay, and Harker, and their study is collectively known as the BFDH theory [4–6]. This theory takes a crystal structure and its symmetry into account and computes the morphology based on the inter-facets distance (d_{hkl}). The BFDH theory works well for relatively simple, isotropic crystalline materials such as metals. In the 1950s, the attachment energy (AE) model was developed by Hartman and Perdok using periodic bond chains (PBCs) and connected nets [7]. The E_{att} was related to the growth rate as reported by Hartman and Bennema. The AE method predicts the growth morphology according to Eq. (1)

$$R_{hkl} \propto E_{att}. \tag{1}$$

CONTACT Yushi Wen ✉ wenys@caep.cn Institute of Chemical Materials, China Academy of Engineering Physics, P.O. Box 919-326, 621900 Mianyang, China.

Color versions of one or more of the figures in the article can be found online at www.tandfonline.com/gmcl.

The external morphology of crystals is predicted using the E_{att} calculation, where E_{att} the energy is released by the addition of a growth slice of thickness d_{hkl} to the surface of a growing crystal and is represented by Eq. (2):

$$E_{\mathrm{att}} = E_{\mathrm{latt}} - E_{\mathrm{slice}}, \tag{2}$$

where E_{latt} is the lattice energy of the crystal, E_{slice} is the energy of a growth slice with thickness d_{hkl}. The growth rate of the crystal face is assumed to be proportional to its E_{att}, i.e., the faces with the lowest E_{att} have the slowest growth, and therefore have the most morphological importance.

In recent years, the AE model has been applied to study the crystal growth and predict the equilibrium morphologies of crystals [8–17]. Winn and Doherty estimated the facet growth rates using the interfacial energies by a set of mathematical equations [8]. The interfacial energies were estimated again using the experimental data of pure solvent and crystal properties. The biggest advantage of their method is that it is computationally inexpensive. Boerrigter et al. applied the Monte Carlo method to model the morphology of fat crystals and aspartame [9]. Their method was capable of accounting the polar nature of faces, showing a difference in the growth rate even in the absence of solvents. Piana and Gale calculated the rates of many types of materials by incorporating events on the surface using molecular dynamics, and then they simulated the growth of a urea crystal of up to the nanometer scale by the kinetic Monte Carlo method [10].

The AE model assumes that the growth of a surface occurs under vacuum condition, and the predictions using this model have been accurate for the crystals grown by sublimation; however, they have not been accurate for the crystals grown from solution, because this model is intrinsically insensitive to the polar nature of facets and the supersaturation during the growth as well as to the solvents and additives. Thus, the aim of this study was to find a method to investigate the solvent effects on the crystal morphology and provide guidance in selecting solvents. A prior prediction may decrease the time and cost in trial and error processes.

1,3,5-triamino-2,4,6-trinitrobenzene ($C_6H_6N_6O_6$, TATB) is a well-known insensitive high explosive. Since its first synthesis in 1887, it is considered as one of the most important energetic materials owing to its unusual insensitivity to high temperatures, shock, and impact [18–20]. In this study, the modified attachment energy (MAE) [11–17] was used to predict the crystal morphologies of TATB in dimethyl sulfoxide (DMSO).

2. Method and simulation details

To account solvent effects, the MAE model developed recently was used [11–17] and it accounts for the effect of the solvent by decreasing the vacuum E_{att} using the solvent-crystal interaction energies.

In the MAE model, the growth rate of a crystal face [*hkl*] is proportional to the modified attachment energy (E^{s}_{att}) as shown in Eq. (3),

$$R_{hkl} \propto E^{s}_{\mathrm{att}}. \tag{3}$$

The $E^{s}{}_{\mathrm{att}}$ accounts for the effect of the solvent by decreasing the vacuum E_{att} using the solvent-crystal interaction energies. The solvent can be assumed to decrease the growth rate and has to be removed from the surface before the crystal facet can grow. This process requires energy and therefore the apparent E_{att} decreases.

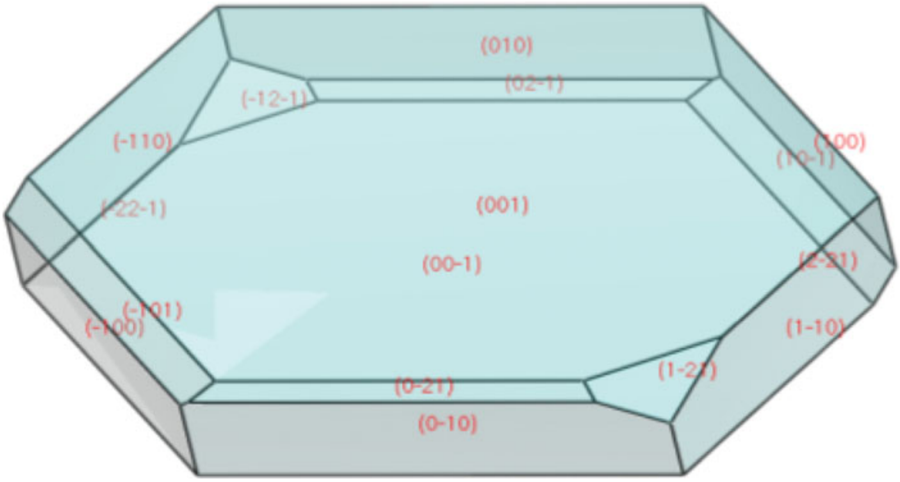

Figure 1. The crystal morphology of TATB in vacuum by AE calculation, with aspect ratio = 4.576, surface/volume ratio = 1.44, unique facets = 16, total facets = 16.

In this study, the interaction energy between the solvent and crystal facets was used to calculate E^{s}_{att} by using Eq. (4):

$$E^{s}_{\mathrm{att}} = E_{\mathrm{att}}\left(1 - \frac{E_{\mathrm{int}}}{E_{\mathrm{att}} + E_{\mathrm{int}}}\right), \tag{4}$$

whereE_{int} is the specific interaction energy between the crystal facet [*hkl*] and the solvent molecules, expressed by Eq. (5),

$$E_{\mathrm{int}} = E_{\mathrm{tot}} - E_{\mathrm{surf}} - E_{\mathrm{solv}}, \tag{5}$$

whereE_{tot} is the total energy of the interactive system comprising a specific crystal surface and solvent molecules.

A TATB model was built according to the experimental data [20, 21], as a triclinic space group *P*-1 with $a = 9.010$ Å, $b = 9.028$ Å, $c = 6.812$ Å, $\alpha = 108.590°$, $\beta = 91.820°$, and $\gamma = 119.970°$, containing two molecules per unit cell.

The AE model was used to predict the crystal morphology in vacuum, providing a list of possible crystal facets with different inherent multiplicities. The TATB surfaces were built by cleaving the TATB crystal parallel to the (*hkl*) plane, which was constructed as a periodic superstructure of 5 × 5 unit cells.

An optimized solvent was placed on this surface, and a vacuum slab with a thickness of 50 Å was built above the solvent layer to eliminate the effect of additional free boundaries on the structure.

Table 1. E_{att} and total facet area (TFA).

hkl	E_{att} (kcal/mol)	TFA (%)	*hkl*	E_{att} (kcal/mol)	TFA (%)
[0 0 1]	− 5.82	31.18	[1 0 −1]	− 19.41	1.36
[0 0 −1]	− 5.82	31.18	[−1 0 1]	− 19.41	1.36
[0 −1 0]	− 18.63	6.24	[0 2 −1]	− 22.36	0.77
[0 1 0]	− 18.63	6.24	[0 −2 1]	− 22.36	0.77
[1 −1 0]	−22.21	5.24	[−1 2 −1]	− 24.01	0.51
[−1 1 0]	− 22.21	5.24	[1 −2 1]	− 24.01	0.51
[−1 0 0]	− 22.09	4.65	[−2 2 −1]	− 23.92	0.02
[1 0 0]	− 22.09	4.65	[2 −2 1]	− 23.92	0.02

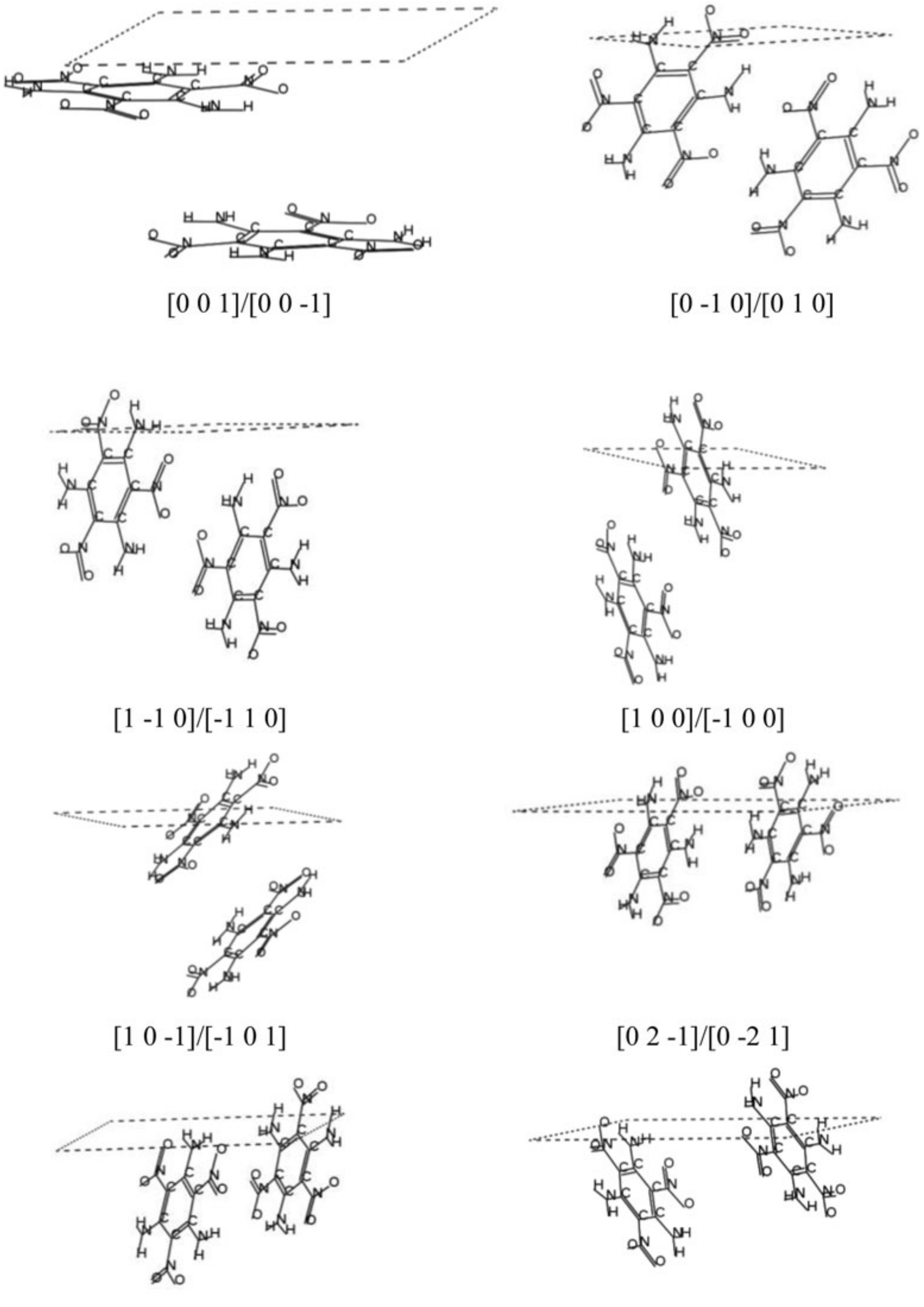

[0 0 1]/[0 0 -1]

[0 -1 0]/[0 1 0]

[1 -1 0]/[-1 1 0]

[1 0 0]/[-1 0 0]

[1 0 -1]/[-1 0 1]

[0 2 -1]/[0 -2 1]

[1 -2 1]/[-1 2 -1]

[-2 2 -1]/[2 -2 1]

Figure 2. Structures of different faces.

Table 2. E_{int} between facet [*hkl*] and solvent molecular (kcal/mol).

hkl	E_{int}	hkl	E_{int}
[0 0 1]	− 9.71	[1 0 −1]	− 8.63
[0 0−1]	− 9.71	[−1 0 1]	− 8.63
[0 −1 0]	− 16.74	[0 2 −1]	− 5.49
[0 1 0]	− 16.74	[0 −2 1]	− 5.49
[1 −1 0]	− 14.28	[−1 2 −1]	− 10.77
[−1 1 0]	− 14.28	[1 −2 1]	− 10.77
[−1 0 0]	− 12.28	[−2 2 −1]	− 4.5
[1 0 0]	− 12.28	[2 −2 1]	− 4.5

E_{tot},E_{surf}, and E_{solv} are calculated via the GGA-BLYP method DNP and basis set, and the AE calculations were performed via the *COMPASS* force field and *Ewald* summation method.

3. Results and discussion

3.1. Crystal habit in vacuum

The result of the crystal shape calculation according to the AE model was found to be similar to the hexagonal cell (Fig. 1). The total number of unique facets is 16, and the total facet area of facet [0 0 1] and its symmetrical facet [0 0 −1] is 62%, and thus these two facets are morphologically more important than the others (Table 1).

3.2. Modified process

The total facet area is determined by its growth speed, and lower growth rate leads to a larger facet area. The facet growth speed is affected by the surface chemistry and topography of the crystal habit faces, which is revealed by the structures of different faces (Fig. 2). A TATB molecule is a near planar structure because of the conjugation effect of benzene ring.

The E_{int} is related to the chosen facet, calculated by Eq. (5) as listed in Table 2. The MAE is calculated by Eq. (4), as shown in Table 3.

3.3 Crystal morphology of TATB in different solvents

According to the above-mentioned MAE model, the crystal morphology and aspect parameter of TATB in DMSO are calculated as shown in Fig. 3.

Figure 3. shows that TATB crystals grow into a hexagonal-flake like shape in DMSO, and the facets such as [1 0 −1] /[−1 0 1], [0 2 −1]/[0 −2 1], [−1 2 −1]/[1 −2 1], and [−2 2 −1]/[2 −2 1] disappear compared to the morphology under vacuum condition (Fig. 1), when

Table 3. The modified attachment energy E^s_{att} (kcal/mol) in solvent.

hkl	E^s_{att}	hkl	E^s_{att}
[0 0 1]	− 2.18	[1 0 −1]	− 13.43
[0 0−1]	− 2.18	[−1 0 1]	− 13.43
[0 −1 0]	− 9.81	[0 2 −1]	− 17.95
[0 1 0]	− 9.81	[0 −2 1]	− 17.95
[1 −1 0]	− 13.52	[−1 2 −1]	− 16.57
[−1 1 0]	− 13.52	[1 −2 1]	− 16.57
[−1 0 0]	− 14.20	[−2 2 −1]	− 20.13
[1 0 0]	− 14.20	[2 −2 1]	− 20.13

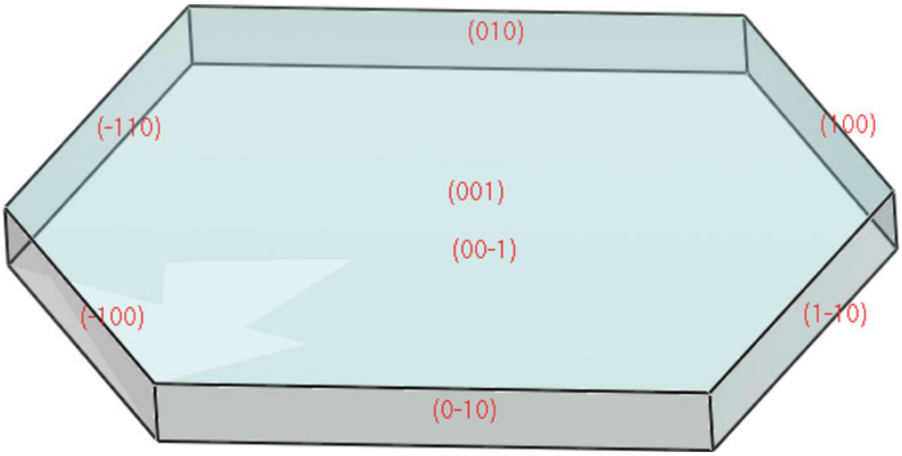

Figure 3. The crystal morphology in DMSO by the MAE calculation. Aspect ratio: 7.628, Total facets: 8.

the solvent effect is taken into account. The value of E_{int} in Table 2 shows that the attractions between the solvent and above-mentioned facets are weaker than those in the other facets. It is intelligible that a weaker solvent-facet interaction will not restrain the attachment behavior of TATB on the chosen facet, and thus the facet grows faster than the others and eventually disappears. In contrast, the stronger attraction between the solvent and a selected facet will restrain the attachment of TATB molecules onto this surface, thus decreasing the growth rate.

TATB was crystallized to compare the calculation result with the experimental data. TATB powder was placed in DMSO, heated, and cooled to isolate TATB crystals. Scanning electron microscope (SEM) image for this sample was recorded, as shown in Fig. 4.

The morphology of TATB is shown in Fig. 4, indicating that our modeling method is in good agreement with the experimental data.

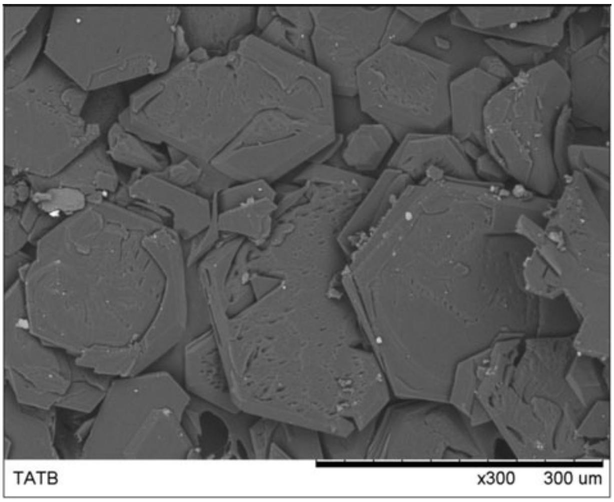

Figure 4. SEM image of the TATB crystals in DMSO.

4. Conclusions

The modified AE method was used to study the morphological behaviors of TATB in different solvents, indicating that TATB crystals grew into a hexagonal-flake shape in DMSO, which is in good agreement with the experimental fact. The high-order facets, observed under vacuum condition simulation, disappeared when the solvent effect was taken into account. Our result indicates that the strength of the interaction between the crystal faces and the solvent molecule varies with the facet types, and a stronger attraction between the selected surface and solvent would restrain and enhance the attachment of TATB molecules onto this surface, decreasing the growth, increasing the surface area. This modified AE method is suitable for predicting the morphological behaviors of TATB and its analogs.

Funding

We greatly appreciate the financial support from the Natural Science Foundation of China (11572296 and 11372292) and the Science and Technology Development Fund of CAEP (2015B0101011).

References

[1] Kundin, J., Yurudu, C., Ulrich, J., & Emmerich, H. (2009). *Eur. Phys. J. B*, *70*, 403–412.
[2] Liu, R. et al. (2013). *Chin. Sci. Bull.*, *58*, 1892–1896.
[3] Duan, X., Wei, C., Liu, Y., & Chonghua, P. (2010). *J. Hazard. Mater.*, *174*, 175–180.
[4] Bravais, A, & de Beaumont, L.É., (1866). *Gauthiers-Villars*, *1*, 17.
[5] Freidel, M. (1907). *Bull. Soc. Fr. Mineral*, *30*, 326–455.
[6] Donnay, J., & Harker, D. (1937). *Am. Mineral*, *22*, 446–467.
[7] Hartman, P., & Perdok, W.G. (1955). *Acta Crystallogr.*, *8*, 49–52.
[8] Winn, D., & Doherty, M.F. (1998). *AIChE J.*, *44*, 2501–2514.
[9] Boerrigter, S.X.M. et al. (2002). *Cryst. Growth Des.*, *2*, 357–361.
[10] Piana, S., & Gale, J.D. (2005). *J. Am. Chem. Soc.*, *127*, 1975–1982.
[11] Kumar, D., & Shastri, N.R. (2014). *Cryst. Growth Des.*, *14*, 326–338.
[12] Liang, Z. et al. (2014). *Comput. Chem. Eng.*, *62*, 56–61.
[13] Qinhua, Y. et al. (2013). *J. Cryst. Growth*, *372*, 193–198.
[14] Clydesdale, G., Roberts, K.J., & Telfer, G.B. (1998). *J. Phys. Chem. B*, *102*, 7044–7049.
[15] Sweegers, C. et al. (2002). *J. Phys. Chem. B*, *106*, 1004–1012.
[16] Beyer, T., Day, G.M., & Price, S.L. (2001). *J. Am. Chem. Soc.*, *123*, 5086–5094.
[17] Walker, E.M., Roberts, K.J., & Maginn, S.J. (1998). *Langmuir*, *14*, 5620–5630.
[18] Talawar, M.B. et al. (2006). *J. Hazard. Mater. B*, *137*, 1848–1852.
[19] Yeager, J.D. et al. (2010). *J. Colloid Interface Sci.*, *352*, 535–541.
[20] Boddu, V.M. et al. (2010). *J. Hazard. Mater.*, *181*, 1–8.
[21] Cady, H.H., & Larson, A.C. (1965). *Acta Crystallogr.*, *18*, 485–496.